Vascular mimetics based on microfluidics for imaging the leukocyte–endothelial inflammatory response

Ulrich Y. Schaff,[a] Malcolm M. Q. Xing,[a] Kathleen K. Lin,[a] Ning Pan,[a] Noo Li Jeon[b] and Scott I. Simon*[a]

Received 8th August 2006, Accepted 2nd January 2007
First published as an Advance Article on the web 23rd January 2007
DOI: 10.1039/b617915k

We describe the development, validation, and application of a novel PDMS-based microfluidic device for imaging leukocyte interaction with a biological substrate at defined shear force employing a parallel plate geometry that optimizes experimental throughput while decreasing reagent consumption. The device is vacuum bonded above a standard 6-well tissue culture plate that accommodates a monolayer of endothelial cells, thereby providing a channel to directly observe the kinetics of leukocyte adhesion under defined shear flow. Computational fluid dynamics (CFD) was applied to model the shear stress and the trajectory of leukocytes within the flow channels at a micron length scale. In order to test this model, neutrophil capture, rolling, and deceleration to arrest as a function of time and position was imaged in the transparent channels. Neutrophil recruitment to the substrate proved to be highly sensitive to disturbances in flow streamlines, which enhanced the rate of neutrophil–surface collisions at the entrance to the channels. Downstream from these disturbances, the relationship between receptor mediated deceleration of rolling neutrophils and dose response of stimulation by the chemokine IL-8 was found to provide a functional readout of integrin activation. This microfluidic technique allows detailed kinetic studies of cell adhesion and reveals neutrophil activation within seconds to chemotactic molecules at concentrations in the picoMolar range.

Introduction

Acute vascular inflammation has been implicated in a diverse set of human diseases including atherosclerosis and psoriasis.[1,2] The initial inflammatory response consists of leukocyte adhesion to the vascular endothelium at sites of infection along post capillary venules.[3] Leukocyte–endothelial interactions proceed as a series of discrete steps that are initiated by selectin bonds that support "rolling". This close contact mediated by selectins allows leukocytes to encounter chemokines presented proximal to the endothelial membrane leading to activation of leukocyte integrins which mediate firm adhesion of the leukocyte to the vessel wall. Finally, arrested leukocytes transmigrate through the endothelium and into the tissue to address the source of inflammation. This multi-step process of adhesion is especially sensitive to the fluid shear stress of blood flow, which provides the driving force that initiates cell rolling and also mechanically influences the process of leukocyte activation.[4] Much of the current knowledge of how fluid shear force regulates the multi-step process of leukocyte recruitment has come from directly imaging the process in a parallel plate flow chamber (PPFC) that mimics the parabolic flow profile in venules.[5–7] In the current study we endeavored to design a microfluidics based shear flow chamber that provides higher throughput and more precise volumetric delivery in quantifying neutrophil activation and adhesion on inflamed endothelium.

In order to construct an *in vitro* model of leukocyte recruitment at least two elements of an inflamed blood vessel wall are required: (1) the substrate of endothelial cells or relevant vascular adhesion molecules and (2) the shear stress which transports leukocytes over the substrate and applies tensile loading to the resulting ligand–receptor bonds between the leukocyte and substrate. The standard PPFC consists of an upper plate on the order of 2 cm in length, assembled above a transparent lower plate that serves as the adhesive substrate. This assembly is positioned above an inverted phase contrast microscope so that the entire process of leukocyte recruitment may be observed. Due to the large cross sectional area of a standard chamber, large volumes of leukocytes and reagents must be continuously pumped through to maintain a venular level of shear stress. For instance, a typical PPFC with a 2 cm $\times$ 300 μm cross section producing a wall shear stress of 2 dynes cm^{-2} consumes upwards of 3 mL of sample liquid per minute. Therefore, these devices have been of limited utility for the study of precious inhibitors, drugs, or antibodies; or for sparse leukocyte types such as monocytes.[8]

Microfluidic channels on the order of 100 μm in height are fabricated by soft lithography from poly(dimethylsiloxane) (PDMS) and are a strategic alternative to the parallel plate flow chamber due to the precision with which a well defined geometry that optimizes leukocyte recruitment can be replicated.[9] For instance, by limiting the cross sectional area we can achieve a reduction in fluidic dead volume between the sample reservoir and the observation channels. This translates to an order of magnitude decrease in the lag time between the

[a]*Department of Biomedical Engineering, University of California, Davis, 451 E. Health Sciences Drive, Davis, CA 95616, USA. E-mail: sisimon@ucdavis.edu; Fax: +1 (530) 754-5489; Tel: +1 (530) 752-0299*
[b]*Department of Biomedical Engineering, University of California, Irvine, Irvine CA 92697, USA*

addition of leukocytes or chemical stimuli to the reservoir and the observation of interaction with the cellular substrate in the channels. Therefore, an increase in leukocyte concentration within the reservoir will immediately be reflected by greater leukocyte flux through the channels.[10] Furthermore, PDMS microfluidic devices can be scaled to match the geometry of small blood vessels and produce defined shear stress and velocity streamline variation along their length. To reap practical benefits from using microfluidics one must overcome several obstacles. Indeed, the standard technique of bonding PDMS to a glass slide by pretreatment with oxygen plasma makes it incompatible with standard culture techniques that involve adhesion of live cells to wet substrates. Also, the prolonged shear stress generated within the narrow inlet tubing commonly used in microfluidics render these devices less useful for the study of shear sensitive leukocytes.

We have designed a microfluidic system that greatly reduces sample size and inlet volume compared to conventional parallel plate techniques, while maintaining compatibility with live cell substrates and high throughput imaging of leukocyte interaction. We demonstrate a device that mates a network of PDMS microchannels to a cell monolayer for the study of inflammatory response of neutrophils (the most common circulating leukocyte). This vascular mimetic microfluidic chamber (VMMC) is designed to precisely control the input concentration of cells or reagents with time and observe leukocyte/monolayer interactions along the channel from the point of entry to exit. We take advantage of this precise sample delivery to determine the rate at which rolling neutrophils arrest in response to activation by a chemotactic stimulus at a defined inlet concentration. In order to confirm that our device yields flow profiles predicted by theory, we modeled the profile of wall shear stress and particle collision rate at the floor of our channels, and used these simulations to predict regions of enhanced neutrophil recruitment that occurred *in vitro*. Downstream from the flow inlet, rolling velocity and recruitment density of neutrophils matched that predicted for a PPFC at an equivalent local shear stress. We present analysis of our PDMS microfluidic system applied to three biological readouts of inflammation: leukocyte capture efficiency, rolling velocity, and the timecourse of leukocyte deceleration to arrest following addition of stimulus.

Experimental

Design

Our design aim was to create a microfluidic device capable of delivering fluid with precisely controlled chemical composition and shear stress to a wide variety of biological substrates.

A significant difference between our microfluidic device and typical PDMS channels is the incorporation of a network of interconnected vacuum channels into the design, which may be connected to a standard vacuum line to provide uniform bonding to any underlying surface. Unlike the standard oxygen plasma treatment of PDMS, vacuum sealing allows reversible bonding to pre-formed, hydrated substrates including living cell monolayers and adsorbed recombinant proteins. To our knowledge this is the first application of vacuum sealing to connect PDMS microfluidics to a pre-existing cell monolayer grown in static culture in a 6-well plate. An important distinction of our vacuum sealed microfluidic system compared to conventional devices is that flow is driven by a syringe pump applying negative pressure to the outlet rather than positive pressure to the inlet. This mode grants two major advantages: the resulting negative pressure enhances the integrity of the vacuum seal and the sample reservoir may be left open to addition of reagents.

A number of important questions relating to the earliest events of acute inflammation may be addressed by controlling the cellular and chemical composition entering a flow chamber in real time. A blunt, shortened 20 gauge needle with 100 μL capacity is press fit directly into the device to serve as a sample reservoir, reducing inlet dead volume to less than 2 μL (Fig. 1); a value three orders of magnitude smaller than a parallel plate flow chamber. Because we use withdrawal pumping and an "on chip" reservoir, volume transfer with micropipette to the open reservoir facilitates rapid addition of cells or reagents into the channel.

Four independent and vacuum isolated flow chambers are integrated into each device and are addressed by sequential connection to a syringe pump and perfused with separate suspensions of leukocytes. This makes it possible to perform four different experimental conditions on each well of a 6-well culture plate. Thus, a total of 24 tests can be applied to a single substrate (Fig. 1). In contrast, a conventional PPFC requires an individual Petri dish or coverslip coated with cells for every experimental condition due its much larger footprint. A second advantage of the small profile of the VMMC is that 3 complete microfluidic devices can be replicated on a single 3 inch silicon master. This yields the practical advantage of batch production and a truly disposable flow chamber that, unlike traditional parallel plate flow chambers, need not accumulate introduced chemicals or microdamage during multiple

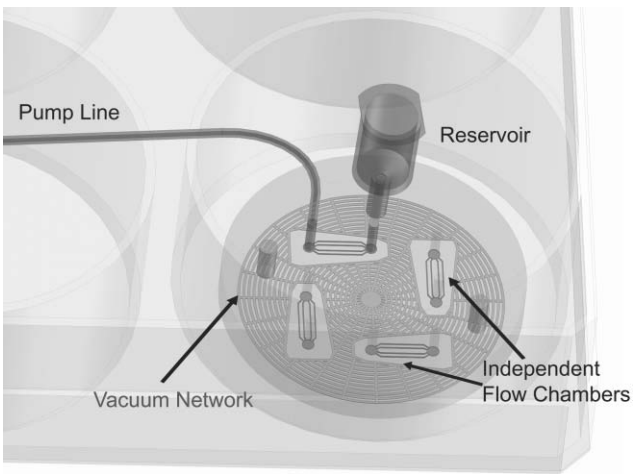

Fig. 1 *Schematic of the vascular mimetic device*. The silicon master pattern produces a flow chamber consisting of four independently operated sets of channels, which are isolated by intervening vacuum lines. Channels are placed within a standard 6-well culture plate in a single well. When adapted to lab vacuum, the interconnected channels on the bottom of the device ensure reversible sealing to a monolayer of cells grown within the 6-well plate, eliminating the need for specialized *in situ* culture techniques.

experiments. After an initial investment of US $100 and 3 h labor to fabricate a silicon master, individual VMMCs requires approximately 15 min of labor and less than US $1 in material as compared to US $400+ for a commercial PPFC.

Each independent flow chamber is composed of 4 parallel channels that are 100 μm in height and 200 μm in width, and are connected to a common inlet and outlet port. This pattern optimizes the balance between reduced sample consumption (narrower channels) and steadiness of pump pressure at flow rates below 1 μL min^{-1} in a parallel plate flow profile. By incorporating four parallel channels to distribute flow, we have increased the ability to address local variations in the substrate (*i.e.* monolayer or protein density) by providing spatially separated observation regions. An experimenter may scan from one channel to another in order to collect averaged data from leukocytes interacting with different portions of a monolayer under the same flow conditions.

In summary, our design eliminates several drawbacks of conventional PPFC or oxygen plasma bonded PDMS microfluidics. It interfaces with a living monolayer, eliminating the requirement to grow an endothelial layer over the course of multiple days, and allowing high throughput analysis of experimental substrates. Our design maintains the low sample volume of microfluidics, and uniquely offers multiple isolated experimental conditions on a single monolayer.

Experimental procedures

Human neutrophils were isolated from whole blood as previously described.[11] ''L-cells'', a mouse fibroblast cell line, transfected to express human E-selectin (L-E cells) were grown on 6-well cultureware as previously described.[12] We defined an ''index'' shear stress (τ_{index} [dynes cm^{-2}]) by eqn (1), assuming a fluid viscosity (μ) of 0.01 dyn s cm^{-2} (1 mPa s) and infinite parallel plate flow conditions, where w is channel width and h is channel height ([cm]) and Q is flow rate ([cm^3 s^{-1}]). Although shear stress varies radially across the flow channel, and true viscosity of our buffer at 37 °C is lower than 0.01 dyn s cm^{-2}, this provides a convenient conversion factor for flow rate to shear stress measures.

$$\tau_{index} = \frac{6\mu Q}{wh^2} \quad (1)$$

Isolated neutrophils, diluted to a concentration of 1.5 × 10^6 mL^{-1} in HEPES buffered saline (110 mM NaCl, 10 mM KCl, 10 mM glucose, 1 mM $MgCl_2$, and 30 mM HEPES (pH 7.35)), were drawn into the microchannels by way of a syringe pump (Harvard Apparatus/Kent Scientific) and visualized using a 20× phase contrast objective within an enclosed 37 °C incubator atop an inverted microscope (Nikon TE200). The flow rate was set to 16 μL min^{-1} corresponding to a shear stress of 2 dyn cm^{-2} (0.2 Pa), which is within the physiological range for leukocyte recruitment (1–6 dyn cm^{-2}).[13] Image sequences from these experiments were digitized by an analog to digital frame grabber (Scion) and recorded for analysis. Neutrophils captured by the L-E monolayer (a confluent layer of murine L-cells expressing human E-selectin that act as a substrate) were identified by their brightness under phase contrast illumination. Adhesion density between 1–6 min was directly measured from captured images while instantaneous velocity was determined by changes in neutrophil centroid position between frames.[14]

In order to characterize the relationship between a local concentration of chemical stimulus and integrin-dependent leukocyte arrest, neutrophils were allowed to accumulate on the L-E monolayer in shear flow at a shear stress of 2 dyn cm^{-2} (0.2 Pa) followed by addition of a defined concentration (1, 0.1, or 0.01 nM) of recombinant human interleukin-8 (IL-8) in HEPES buffered saline. As an index of neutrophil response to these chemokines, we measured the fraction of total neutrophils transiently arrested to the L-E monolayer as a function of time. As a second, more discrete measure of neutrophil activation, we calculated the instantaneous velocity of neutrophils over the course of 60 s as they decelerated in response to chemokine.

Fabrication

Master molds for the devices were fabricated by patterning SU-8 50 photoresist with a thickness of 100 μm as described previously.[15] By casting PDMS (Sylgard 184) prepolymer over these etched silicon masters, PDMS replicas were produced as described previously.[15] Flow and vacuum access holes were punched directly into PDMS replicas using a symmetrically sharpened 16 gauge needle.

CFD

In the microvasculature, leukocytes initially contact the endothelial lining of blood vessels after becoming marginated to the walls by collisions with high density red blood cells. In contrast, contact between leukocytes and the substrate in our microfluidic channels occurs as a result of gravitational sedimentation and flow directed collisions, which may be accurately modeled based on geometry. We used CFD to produce steady state models of fluid streamlines, neutrophil pathlines, and substrate shear stress. In addition, we produced dynamic simulations of chemical transport within the flow channel and neutrophil collisions with the substrate. A three dimensional model of our PDMS device was imported into ANSYS/Preprocessor from CAD (Autodesk, San Rafel CA), divided into regular brick elements, and then exported to ANSYS/CFX. A steady laminar solution was executed and, for particle collision and chemical diffusion modeling, a two-way coupled method was employed in CFX.[16] In accord with our experimental condition, simulation parameters specify an inlet mass flow rate of 0.267 mg s^{-1} with a fluid viscosity of 0.88 mPa s and assume symmetrical surfaces and boundary conditions within the PDMS. The thickness of the PDMS used to construct our flow chambers is 15 mm or 150 times the height of the channels, rendering vertical deformation of flow channels due to internal negative pressure negligible; an assumption supported by a lack of observed lateral deformation in the channel side-walls during device operation. Because of this negligible change, flow could be accurately modeled by assuming positive pressure, assigning the outlet port to a relative pressure of 0 dyn cm^{-2}. Solid surfaces were constrained to fulfill the no-slip condition. For particle-surface collision simulations fluid density is assumed to be 1 g mL^{-1}

and neutrophil density 1.086 g mL^{-1} with a particle size of 8.2 μm and a gravitational acceleration of 9.8 m s^{-2}.

Results and discussion

Device characterization

Parallel plate studies in which leukocyte–substrate adhesion is quantified by video microscopy typically yield two types of time variant data: the number of leukocytes that attach to the surface per unit area (recruitment density) and the distance that the average adherent leukocyte moves across the substrate per unit time (rolling velocity).[12] This data is typically collected by microscopic observation of random regions of the parallel plate substrate, implicitly assuming that flow profile is constant across the channel and leukocyte interaction is independent of spatial location.[17] However, within the reduced dimensions of our microfluidic system, wall shear stress will decrease toward the channel side-walls and may vary along the length of the channels. It is important that our device provides consistent conditions for leukocyte-substrate interaction, and therefore we characterized the spatial dependence of shear stress and leukocyte recruitment within the flow channels.

Shear stress modeling

Approximating the flow channels as an infinite parallel plate with fluid flowing through at a rate of 16 μL min^{-1} flow rate yields a predicted shear stress of 2 dyn cm^{-2} (0.2 Pa), a value on the lower end of the physiological range of 1–6 dyn cm^{-2} for venous circulation.[13] To account for deviations from this ideal model, we modeled the wall shear stress within our flow chamber at the applied experimental flow rate (16 μL min^{-1}) using ANSYS/CFX. Taking into account that the flow channels are not infinite in width reveals a nearly parabolic profile with an average shear stress of 1.81 dyn cm^{-2} that reaches a maximum of 2.4 dyn cm^{-2} at the centerline (Fig. 2A). A decline is predicted in the peripheral 25% of channel area closest to the sidewalls where lower plate stress falls from 1.49 dyn cm^{-2} to zero at the no slip boundary at the channel sidewall. We have previously reported that neutrophil arrest increases by 7%, and velocity decreases by 7% when shear stress drops from 2 to 1 dyn cm^{-2} on L-cell monolayers expressing E-selectin. We anticipate that velocity and adhesion density in the core 75% of the flow channel should not deviate by more than 5% from the mean (average τ = 2.11 dyn cm^{-2}).[12]

Radial consistency in recruitment

In order to confirm this predicted correlation between adhesion parameters and changes in wall shear stress, we measured neutrophil recruitment density at radial positions perpendicular to the axis of flow. The VMMC is capable of interfacing with a monolayer of primary human endothelial cells (*i.e.* human umbilical vein endothelial cells), closely mimicking the lining of an inflamed blood vessel. However, in order to characterize neutrophil recruitment in the absence of activating chemokines, we assembled the microfluidic device above a simpler model substrate: a monolayer of L-cell expressing E-selectin, and infused 1.5 × 10^6 neutrophils mL^{-1} in an assay buffer. At an index shear stress of 2 dyn cm^{-2} neutrophils are captured by E-selectin and roll along the surface without coming to arrest. Neutrophil adhesion density, rate of accumulation, and rolling velocity remained constant in the radial direction across the core 150 microns of each flow channel (Fig. 2B). Within 25 microns of the wall, where shear stress was estimated to decline by an average of 56% from the core, mean velocity showed no significant decrease (actually an increase of 12% Fig. 2B) while adhesion density was modestly suppressed. This stability of rolling velocity near the wall is

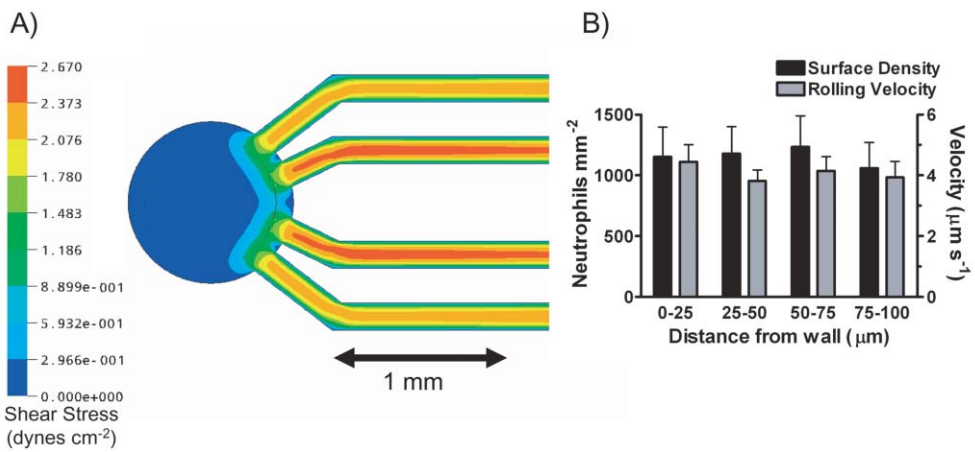

Fig. 2 *Characterization of neutrophil recruitment within the channels by computational fluid dynamics and experiment*. (A) A computed map of wall shear stress distribution reveals that stress reaches its steady state profile almost immediately upon entry at an inlet flow rate of 16 μL min^{-1}. The shear stress profile within the inner flow branches is 4% higher than the analogous profile on the outer branches, a deviation with minimal impact on leukocyte interaction in the physiological range. Similarly, shear stress within the core 100 and 150 microns of each branch remains within 8.5% and 30% of the respective average stress. (B) Measurements of neutrophil rolling velocity and recruitment density were separated into eight 25 μm lanes based on radial distance from the channel sidewall. Within the bounds of error, velocity remains constant except nearest to the channel walls, while recruitment density is constant across the width of the channel. Error bars are based on standard error from n = 9 experiments with >6 neutrophil velocity measurements each. Recruitment densities are based on the average number of neutrophils in 6 random fields over the initial 6 minutes of flow perfusion.

likely enabled by a diminished efficiency of selectin bond formation at low shear stress, which has previously been reported to elicit transient detachments from the substrate.[18] In summary, the key indices of velocity and recruitment density remain consistent across the width of the flow channels, even within 25 microns of the side-walls where shear stress is predicted to decrease.

Basis for radial velocity distribution

Capture efficiency and rolling velocity of leukocytes on selectins does not scale linearly with shear stress or collision frequency. For instance, neutrophil rolling velocity is relatively constant over a range of venular shear stress (1–6 dyn cm^{-2}).[13,19] This may correlate with the fact that the lifetime of selectin bonds only changes by a factor of two over an order of magnitude change in pulling force.[20,21] At very low shear stress (<0.4 dyn cm^{-2}) neutrophils do not interact effectively with selectins, resulting in an increase in apparent rolling velocity due to transient detachments.[22] Indeed, in this device we measured a higher average rolling velocity at an index shear of 0.1 dyn cm^{-2}, compared to 2 dyn cm^{-2} (data not shown). Consistent with this observation, the standard deviation of instantaneous velocity in neutrophils rolling within 25 μm of the wall was 70% greater than that found in the center of the channel (deviation of 4.81 *vs.* 2.84 μm s^{-1} respectively). This non-linear shear dependence of selectin interactions explains the lack of variation in velocity near the channel center where shear stress is approximately constant, and the stability of mean velocity within 2 cell diameters of the wall where shear stress approaches zero.

Entrance flow disturbance enhances neutrophil recruitment

As fluid containing suspended leukocytes enter the VMMC, flow must change direction from perpendicular at the chamber entrance to parallel with the substrate along the channels. Because this unintended flow disturbance may alter leukocyte recruitment along the length of the VMMC, we produced a computational model of fluid streamlines that result from 16 μL min^{-1} flow within the VMMC. Although the previously modeled shear stress profile is nearly constant along the length of the channels (Fig. 2A), the streamline model predicts a substantial downward velocity component near the entrance and exit where flow changes its direction from parallel to perpendicular to the surface of the flow chamber (Fig. 3A). A requirement for leukocyte capture is that adhesion receptors physically engage ligands on the substrate, and thus any vertical velocity component can dramatically enhance local adhesion density.

In order to examine the relationship between hydrodynamics and observed neutrophil recruitment, we modeled the flow paths of 1000 randomly placed neutrophils at the entrance to the flow channel (Fig. 3A). We confirmed the fidelity of the computational model to predict flow in the VMMC by measuring the velocity of suspended 10 micron fluorescent particles, finding that the channel centerline velocity was within 1% of the computed maximum neutrophil

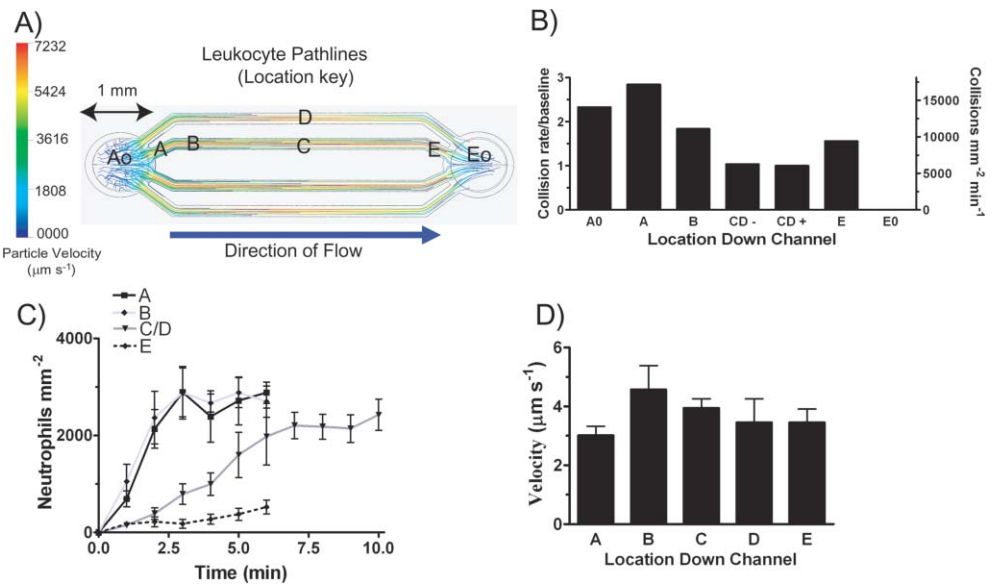

Fig. 3 *Neutrophil capture, pathline, and rolling velocity versus position down a channel.* (A) Neutrophils were simulated as buoyant spheres with an 8.25 μm diameter in order to predict the spatial rate of initial collision with the substrate. (B) The rate of collisions at the locations mapped in Fig. 3A (labeled A–E) are normalized by the collision rate at the central section of the channel. Notably, collisions are greatly enhanced at the entrance (A, B) and upstream from the entrance (A_0) while the rate in the first half (C/D +) and second half (C/D −) of the straight central flow channels are within 3% of each other. There are absolutely no collisions downstream from the exit from the channel region (E_0) due to separation of streamlines from the surface. (C) The density of neutrophil adhesion to the substrate at the indicated locations is displayed at 1 min intervals. Recruitment differences between positions A/B and C/D are statistically significant (t-test $p < 0.05$) from 1–5 min, while differences between C/D and F are significant between 2–6 min. Note that data for position C/D is extended to show a plateau in recruitment after 7 min similar to positions A and B. (D) Velocity at the mapped locations is representative of $n > 4$ separate experiments each based on at least 10 traces of rolling neutrophils. All error bars are based on standard error from the average velocity measured in each experiment.

velocity (7288 $\pm$ 399 μm s^{-1} *vs.* 7232 μm s^{-1} respectively). As suggested by the entrance streamlines, the flow pathline model revealed a pronounced asymmetry in predicted collision density in the first 400 microns of channel length as compared to regions further down the channel. According to the simulation, 3 times the number of neutrophils per unit area first collided with the substrate in this entrance region compared with the fully developed flow region at the channel center (Fig. 3B). After the initial 400 microns (about 50 cell diameters) from the undeveloped fluid profile at the channel entrance and exit, neutrophils sedimented under gravity on the lower substrate at a constant surface density. Neutrophils are not depleted from the perfusion buffer by the time it reaches the channel outlet as neutrophils in the upper streamlines flow through the channel without engaging the bottom plate. Based on the simulation, 19% of inlet neutrophils collided in the entrance region, 56% collided in the remaining channel surface area, and 25% were perfused through the system without collision. Assuming a constant efficiency of adhesion, our simulations predict enhanced adhesion density near the entrance bend which levels off to a constant number in the middle of the channel. This modeling provides a benchmark to compare efficiency of neutrophil capture and arrest with their dependence on biological parameters such as activation state within the VMMC. A future innovation will be the design of a shallow angle of flow impingement onto the substrate to achieve a reduction in pathline collisions at the entrance region and more gradual transition from entrance to channel.

Mid-channel recruitment is spatially consistent

As predicted, recruitment density increased at a much greater rate near the entrance to the flow channels (Fig. 3C position A), reaching a steady state value at around 3000 neutrophils mm^{-2}. This enhanced capture was accompanied by a 24% reduction in rolling velocity compared to the midpoint (Fig. 3D position C). Because neutrophils continued to roll towards the channel exit following initial capture, the density of recruited neutrophils remained elevated at a position 400 microns downstream from the area of maximum collision rate (Fig. 3C position B). Interestingly, neutrophil recruitment density was substantially depressed at the channel exit (position E) compared with the channel midpoint without a significant difference in velocity. On the other hand, the density of neutrophil capture was spatially consistent, reproducible, and linearly increased with time at the midpoint of the flow channels (Fig. 3C position C/D). This result indicates that at the midpoint of the flow channels, a constant number of neutrophils per unit time are captured by the adhesive surface until recruitment reaches the steady state value after 7 min.[17] Mean leukocyte rolling velocity was not significantly different between the inner and outer sets of channels (Fig. 3D position D *vs.* E). The results of our modeling and experiments suggest that measurements of neutrophil recruitment density and velocity are remarkably consistent throughout the narrow flow channels, and that consistency is optimized at the center and core of the flow channels where entrance and wall affects are negligible.

Fluidic basis of leukocyte recruitment pattern

The enhanced capture of neutrophils at the entrance region and the profile of neutrophil rolling velocities are only partially explained by our CFD models of shear stress and pathline. Although the calculated shear stress profile at the channel entrance is nearly identical to the mid-channel profile, experiments showed that neutrophil rolling velocity is substantially depressed at the entrance. The curvature of the streamlines as the flow transitions from vertical to horizontal at the entrance imparts a downward force on particles in this region that may serve to increase the deformation of the neutrophils, increasing the contact area with the substrate. We have recently reported that a force driven increase in contact area can increase selectin bond formation and the probability of capture, while decreasing rolling velocity in a mathematical simulation of leukocyte deformation and adhesion[23,24] Thus, not only are more neutrophils delivered to the surface at the channel entrance, but each cell is more likely to tether to the monolayer. This mechanism may also begin to explain the reduced recruitment density near the channel exit point, where separating streamlines reduce contact force, and thus capture efficiency, despite a slightly elevated density of predicted neutrophil collisions. Thus, the changes in flow direction at the entrance and exit of the flow channels are analogous to those in the branching microcirculation where impinging flow enhances leukocyte recruitment.[25]

In conclusion, there is agreement in the modeling and experimental data showing that the probability of leukocyte adhesion is strongly enhanced when fluidic streamlines are compressed. On the other hand, predicted variation in shear stress down the flow channels did not produce significant gradients in neutrophil recruitment or rolling velocity. This consistency of rolling velocity combined with a well defined pattern of leukocyte recruitment and shear stress makes the VMMC an ideal system for direct observation of the multistep process of leukocyte adhesion and analysis of the biological drivers of recruitment.

Neutrophil activation *via* binding of chemokine

Because of its low sample size, small volume, and multichannel design the VMMC provides an ideal platform for measuring the time kinetics of neutrophil adhesion in response to an infusion of chemokine. Therefore we applied the VMMC to this problem, as a means of validating the microfluidic technique and probing the spatial requirement of chemokine mediated arrest. Our goals were to determine the precise dose of chemokine necessary to cause a rolling neutrophil to arrest and the rate of neutrophil deceleration upon activation. Both of these goals are attainable due to the well characterized properties of the flow channels and the negligible dead volume within the microfluidic system.

In order to transition from rolling to arrest, integrins on the surface of an adherent neutrophil must become activated, shift into a high affinity conformation, and bind integrin ligands (*i.e.* ICAM-1) on inflamed endothelial cells.[26] Chemokines such as IL-8 are known to bind to G-protein coupled receptors on the neutrophil surface where they trigger an intracellular signal cascade that induces a shift to high affinity.[27] As a

readout of chemokine driven integrin activation, we measured the instantaneous velocity of rolling neutrophils on L-cell monolayers stably expressing physiological site density of E-selectin after exposing them to a defined concentration of IL-8 loaded into the inlet reservoir.[6,28] Because active β2-integrins bind ligands such as albumin present on the L-E monolayer which mediate firm adhesion of neutrophils to the surface, activation is accompanied by a time dependent decrease in average neutrophil rolling velocity. Instantaneous velocity data, derived from video frames 0.25 s apart, provides a sub-second optical readout for integrin activation and cell deceleration. As an index of adhesion efficiency, we also derived the percentage of total surface adherent neutrophils that became arrested (average velocity <0.4 μm s^{-1}) in 5 s intervals. The percent arrest of neutrophils reflects with high sensitivity changes in the activation of integrin bonds that provide the adhesion strength in shear flow.

Dynamics of neutrophil deceleration within microfluidics

IL-8 was introduced into the flow stream in real time by directly replacing the sample reservoir volume (*i.e.* less than 5 μL residue clinging to the reservoir walls) with buffer containing a known concentration of the chemokine. Infusion of 1 nM IL-8, a concentration predicted to occupy ~50% of IL-8 receptors on a neutrophil at equilibrium, resulted in a 50% drop in neutrophil velocity within 8.25 s (Fig. 4A). This velocity decline correlated with a transition to stable arrest in virtually all neutrophils for a duration of ~1 min (Fig. 4A). The percentage of arrested neutrophils approaches 100% following 15 s of chemokine exposure and remains at this level. A similar drop in velocity was seen in neutrophils exposed to 0.1 nM IL-8 after 12 s which corresponds to a delay of 3.75 s from the higher chemotactic dose. At a concentration of 0.1 nM IL-8, corresponding to 20% of β2-integrins in the active state, 76% of neutrophils become arrested, but the majority revert to a rolling phenotype 50 s after the initial decline in velocity (Fig. 4B). The percentage of arrested neutrophils also declines following exposure to 1 nM IL-8, but the majority remain adherent after 3 min. This weakening of adhesion strength correlates with a reversibility in high affinity β2 integrin as reported for neutrophils exposed to soluble IL-8 over the same timecourse.[29] In contrast, exposure to a concentration of 0.01 nM or lower IL-8 had no detectable impact on neutrophil arrest efficiency over the course of 3 min.

Neutrophil arrest to an L-E monolayer is dependent on the activation of the β2-integrin Mac-1, which is rapidly upregulated on the plasma membrane upon neutrophil activation. Mac-1 recognizes a diverse set of ligands including collagen and albumin that are expressed on L-E cells, which otherwise lack expression of the prototypic counter-receptor ICAM-1 found on inflamed endothelial cells.[3,14] We confirmed that anti-Mac-1 but not control IgG abrogates neutrophil arrest (Fig. 4B). Taken as a whole, the data confirm that a threshold dose of chemotactic stimulus is necessary to initiate Mac-1 mediated deceleration in response to IL-8. Further, the extent and reversibility of adhesion is dependent on time and stimulus concentration.

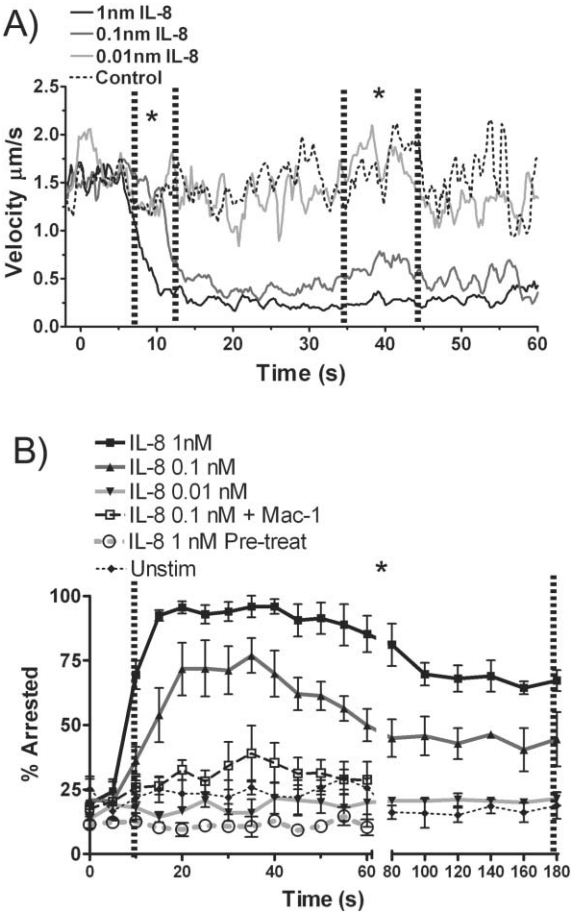

Fig. 4 *Optical detection of the kinetics and molecular specificity of neutrophil velocity and arrest*. Time 0 on all kinetic measurements is adjusted to the moment when chemokine first enters the flow channel; 5 s after a change in reservoir concentration. (A) A plot of the average neutrophil rolling velocity following influx of buffer containing a high concentration (1 nM), low concentration (0.01 nM), or threshold concentration (0.1 nM) of IL-8. In order to smooth the jagged deceleration of transiently detached neutrophils, instantaneous velocities higher than 4 microns s^{-1} are excluded from the running average. Asterisks indicate areas of significant difference between 1 nM and 0.1 nM IL-8 stimulation ($p < 0.05$). (B) A plot of the average percentage of neutrophils that are arrested to an L-E (E-selectin) monolayer following IL-8 infusion. Arrest triggered by 0.1 nM IL-8 is significantly less than that triggered by 1 nM IL-8 at all times between the hash-marks denoted with an asterisk ($p < 0.05$). Antibody against Mac-1 is capable of blocking arrest triggered by this threshold IL-8 dose to the point where it is not significantly different than uninhibited control. Some monolayers were pretreated with 1 nM IL-8 for 5 min with no significant impact on neutrophil arrest. Timecourses for 1 nM, 0.1 nM, and 0.01 nM IL-8 are extended to show a decrease in adhesion strength toward baseline. Error bars indicate standard error based on at least $n = 3$ experiments per time point.

Modeling chemokine transport in the microfluidic channel

In order to compare the predicted mass transport kinetics of IL-8 with the time course of neutrophil activation and arrest, we modeled the dynamics of chemokine diffusion based on a step change in input concentration at a continuous flow rate of 16 μL min^{-1} (Fig. 5A). Since the input reservoir fluid is entirely drained and replaced with a defined concentration of

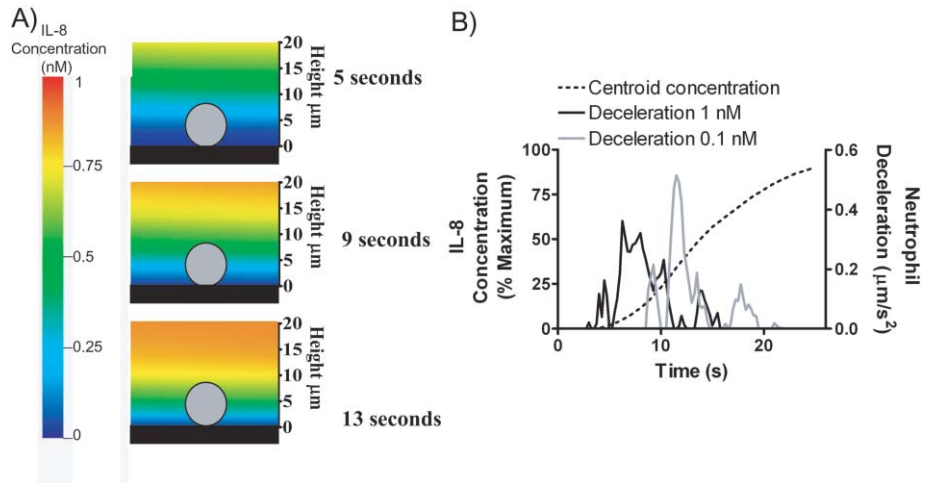

Fig. 5 *Transport and neutrophil deceleration during activation with chemokine*. (A) A plot of simulated IL-8 concentration near the flow channel floor at three time points. A circle the same size as a neutrophil is included to provide a frame of reference. IL-8 is first convected to the center of the flow channel, then diffuses outward toward the neutrophils attached to the chamber floor. (B) A plot of the estimated timecourse of IL-8 concentration at the center (4 µm from the floor) of a rolling neutrophil at the midpoint of the flow channel is overlaid with a plot of the averaged neutrophil deceleration. Because the boundary conditions scale with inlet concentration, the concentration isotherms for 1 nM, 0.1 nM, and 0.01 nM IL-8 are identical.

IL-8, this is an accurate assumption. At the channel midpoint, the simulation predicted a 9 s delay from the initial entry of chemokine into the channel until the concentration 8 µm (one cell diameter) above the channel floor reaches 50% of maximum (Fig. 5A). Infusion of a fluorescent tracker at the reservoir to image the kinetics of diffusion confirmed that chemokine first enters the core of the flow channel then diffuses to the sidewalls along a time course consistent with the simulation, and further indicated an average time of 5 s from infusion to initial detection of core fluorescent signal. Thus, a total of 14 s elapses between the change in reservoir composition and when the apex of each neutrophil is exposed to half maximal chemokine levels. Comparing the velocity response of the average neutrophil with the simulated chemokine diffusion resulting from influx of 0.1 nM IL-8 we observe that neutrophils begin to exhibit deceleration upon exposure to 0.05 nM IL-8 at the cell midpoint. (Fig. 5B) The deceleration curve for 1 nM IL-8 is shifted 3.75 s earlier than 0.1 nM IL-8, which is consistent with an activation threshold of 0.05 nM. An estimate of the number of IL-8 receptors occupied at 0.05 nM is made by considering that the K_D (receptor dissociation constant) is 1 nM for IL-8.

$$\frac{[RL]}{[R]} = \frac{[L]}{[L]+K_D} \quad (2)$$

Thus, this threshold concentration corresponds to ~5% of IL-8 receptors occupied by ligand as derived from eqn (2), where [R] is the total concentration of receptors, [L] is the input concentration of IL-8, and [RL] is the concentration of receptors bound to IL-8. Based on average velocity curves, maximum deceleration of neutrophils occurs 3 s following exposure to 0.05 nM IL-8 and the initial onset of deceleration. This assay of the functional response of neutrophil integrins to chemokine activation is the most sensitive direct measure of adhesion response currently available. Thus, by defining the chemical and shear environment of the neutrophil and recording rolling velocity, we can measure integrin activation at levels below the detection limit of established techniques. Notably, when either 0.1 nM or 1 nM IL-8 is perfused into the flow channels, neutrophils begin to decelerate when less than 0.01 nM IL-8 diffuses within 1 micron of the lower surface (Fig. 5B). This amount of IL-8 is incapable of activating neutrophil arrest as previously indicated in Fig. 4. These adhesion data (Fig. 4B) also show that pre-incubation of L-E monolayers with a high dose (1 nM) of IL-8 is not sufficient to trigger activation of neutrophil arrest through adsorption of chemokine to the apical surface. We conclude that rolling neutrophils begin to respond to IL-8 binding receptors substantially above the point of cell contact with the substrate. These data suggest that such surface presentation of IL-8 on the apical glycocalyx of endothelial cells, such as prescribed in the paracrine model of leukocyte recruitment, is not requisite for neutrophil arrest.[30] Soluble IL-8 at a mean concentration of 0.05 nM was fully competent to trigger maximal neutrophil deceleration in the presence of an integrin ligand within 3 s of exposure. It should be noted that 0.05 nM IL-8 is somewhat higher than the average plasma concentration (~0.02 nM) reported in patients with bacterial sepsis whose tissues experience extremely high neutrophil recruitment.[31] This suggests that selective association of IL-8 with cells or elevated local concentrations of IL-8 at sites of tissue injury can produce robust neutrophil adhesion and tissue recruitment.

Proposed timecourse for IL-8 triggered arrest

By modeling the IL-8 stimulation and correlating this with neutrophil adhesion kinetics we have established the correlation between the number of IL-8 molecules available and neutrophil arrest during rolling on E-selectin. A threshold concentration of ~0.05 nM IL-8 is sufficient to signal activation of Mac-1 and deceleration within 3 s. Over the

next 10 s, a period of adhesion strengthening results in peak shear resistance and increased adhesion efficiency. Furthermore, at lower levels of stimulation (*i.e.* <0.1 nM IL-8), we hypothesize that deactivation of Mac-1 results in a decline in bond strength and neutrophil detachment within ~50 s post-exposure. The observed weakening of adhesion strength may provide an explanation of why leukocytes pre-treated with low concentration of soluble chemokines fail to arrest on competent surfaces.[32] We conclude that exposure to chemokine must occur within a critical window (*i.e.* ~50 s) of integrin ligation in order to facilitate arrest. Taken together, we conclude that homing of a neutrophil at precise location of inflammation in the vasculature involves temporal coordination of both the chemotactic stimuli and accessibility of integrin ligands.

Conclusions

We have developed and validated a vacuum bonded microfluidic system that is broadly applicable to the study of temporal and spatial analysis of cell interaction with a biological substrate, and requires only standard laboratory equipment to operate. Based on a combination of computational simulations of shear flow and molecular diffusion combined with optical imaging of the kinetics of neutrophil adhesion at typical video collection rates, we conclude that threshold concentrations of soluble IL-8 can trigger β2 integrin dependent arrest within seconds. Based on our previously reported relation between chemokine concentration and integrin activation, we estimate that as few as 15 000 active β2 integrins on the surface of a neutrophil are capable of effecting arrest.[29] The reversibility of adhesion strength following chemokine exposure reveals that neutrophil recruitment from the circulation requires precise cooperation between chemotactic signal and the ligation and activation of integrins.

Acknowledgements

This research was funded by the NIH (R01 AI47294, T32 AI060555), and an NSF funded Center for Biophotonics and Science Technology grant.

References

1 P. Libby, *Nature*, 2002, **420**, 868–874.
2 J. G. Krueger, *J. Am. Acad. Dermatol.*, 2002, **46**, 1–23 quiz 23–26.
3 R. Alon and S. Feigelson, *Semin. Immunol.*, 2002, **14**, 93–104.
4 M. B. Lawrence, L. V. McIntire and S. G. Eskin, *Blood*, 1987, **70**, 1284–1290.
5 J. V. Forrester and J. M. Lackie, *J. Cell Sci.*, 1984, **70**, 93–110.
6 M. B. Lawrence and T. A. Springer, *Cell*, 1991, **65**, 859–873.
7 M. B. Lawrence and T. A. Springer, *J. Immunol.*, 1993, **151**, 6338–6346.
8 D. C. Brown and R. S. Larson, *BMC Immunol.*, 2001, **2**, 9.
9 G. M. Whitesides, E. Ostuni, S. Takayama, X. Jiang and D. E. Ingber, *Annu. Rev. Biomed. Eng.*, 2001, **3**, 335–373.
10 G. S. Fiorini and D. T. Chiu, *Biotechniques*, 2005, **38**, 429–446.
11 S. I. Simon, A. R. Burns, A. D. Taylor, P. K. Gopalan, E. B. Lynam, L. A. Sklar and C. W. Smith, *J. Immunol.*, 1995, **155**, 1502–1514.
12 S. I. Simon, Y. Hu, D. Vestweber and C. W. Smith, *J. Immunol.*, 2000, **164**, 4348–4358.
13 M. L. Smith, M. J. Smith, M. B. Lawrence and K. Ley, *Microcirculation*, 2002, **9**, 523–536.
14 O. Abbassi, T. K. Kishimoto, L. V. McIntire, D. C. Anderson and C. W. Smith, *J. Clin. Invest.*, 1993, **92**, 2719–2730.
15 F. Lin, W. Saadi, S. W. Rhee, S. J. Wang, S. Mittal and N. L. Jeon, *Lab Chip*, 2004, **4**, 164–167.
16 W. Zhong and M. Q. Xing, *J. Colloid Interface Sci.*, 2004, **275**, 264–269.
17 Y. Zhang and S. Neelamegham, *Biophys. J.*, 2002, **83**, 1934–1952.
18 S. Chen and T. A. Springer, *Proc. Natl. Acad. Sci. U. S. A.*, 2001, **98**, 950–955.
19 E. Evans, A. Leung, V. Heinrich and C. Zhu, *Proc. Natl. Acad. Sci. U. S. A.*, 2004, **101**, 11281–11286.
20 E. B. Finger, K. D. Puri, R. Alon, M. B. Lawrence, U. H. von Andrian and T. A. Springer, *Nature*, 1996, **379**, 266–269.
21 S. I. Simon and C. E. Green, *Annu. Rev. Biomed. Eng.*, 2005, **7**, 151–185.
22 M. B. Lawrence, G. S. Kansas, E. J. Kunkel and K. Ley, *J. Cell Biol.*, 1997, **136**, 717–727.
23 D. B. Khismatullin and G. A. Truskey, *Microvasc. Res.*, 2004, **68**, 188–202.
24 M. R. King, R. Sumagin, C. E. Green and S. I. Simon, *Math Biosci.*, 2005, **194**, 71–79.
25 K. A. Lamkin-Kennard, J. Y. Chuang, M. B. Kim, I. H. Sarelius and M. R. King, *Biorheology*, 2005, **42**, 363–383.
26 K. Ley, *Immunol. Rev.*, 2002, **186**, 8–18.
27 N. Hogg and B. Leitinger, *J. Leukocyte Biol.*, 2001, **69**, 893–898.
28 J. A. DiVietro, M. J. Smith, B. R. Smith, L. Petruzzelli, R. S. Larson and M. B. Lawrence, *J. Immunol.*, 2001, **167**, 4017–4025.
29 A. F. Lum, C. E. Green, G. R. Lee, D. E. Staunton and S. I. Simon, *J. Biol. Chem.*, 2002, **277**, 20660–20670.
30 K. D. Patel, E. Lorant, D. A. Jones, M. Prescott, T. M. McIntyre and G. A. Zimmerman, *Behring Inst. Mitt.*, 1993, 144–164.
31 C. Marie, C. Fitting, C. Cheval, M. R. Losser, J. Carlet, D. Payen, K. Foster and J. M. Cavaillon, *Infect. Immun.*, 1997, **65**, 865–871.
32 R. Shamri, V. Grabovsky, J. M. Gauguet, S. Feigelson, E. Manevich, W. Kolanus, M. K. Robinson, D. E. Staunton, U. H. von Andrian and R. Alon, *Nat. Immunol.*, 2005, **6**, 497–506.

